Ultraviolet-Assisted Release of Microelectromechanical Systems From Polyimide Sacrificial Layer

Javaneh Boroumand Azad, Imen Rezadad, Robert E. Peale, Justin W. Cleary, and Kurt Eyink

***Abstract*— Process heating of microelectromechanical systems (MEMSs) devices hardens polyimide sacrificial layers, complicating the final release and lowering yield for delicate structures. This paper reports ultraviolet (UV)-assisted release, which is demonstrated on an MEMS cantilever fabricated by an eight-mask photolithographic process. A commercial co-developable polyimide ProLift 100 (Brewer Science) sacrificial layer was used. The process subjects the device to multiple heat treatment steps. Both wet chemical etching and dry reactive ion etching were explored. During the former, large sheets of hardened polyimide floated free of the substrate to damage delicate MEMS structures. The latter is typically slow, so that grass appears during long exposures to plasma ions. The solution reported here is UV exposure prior to release. Optical constants of the sacrificial layer material, which were baked to simulate thermal histories during various fabrication steps, were measured to understand the effectiveness of UV exposure. Wet and dry etch rates were measured as a function of UV dose. Finally, the advantages of UV pretreatment were demonstrated during the release of actual MEMS cantilevers. [2015-0193]**

***Index Terms*— Microelectromechanical systems, semiconductor devices, polyimides, release, ultraviolet, sacrificial layer.**

I. Introduction

MICROELECTROMECHANICAL systems (MEMS) frequently employ moveable structures built on a sacrificial layer, which is dissolved or etched away at the end of the fabrication process [1]–[9]. Example devices include suspended cantilevers anchored at one end or bridges fixed at both ends [10]–[14]. Spin-on polyimide is a common sacrificial material [15]–[19]. However, the more this material is heated, the harder it becomes, which complicates the release after multi-step processing [20]–[26]. This paper presents a means of releasing MEMS structures from a hard-baked polyimide sacrificial layer.

Manuscript received July 8, 2015; accepted July 24, 2015. This work was supported by Florida High Technology Corridor under the I-4 Program. The work of J. W. Cleary was support by the Air Force Office of Scientific Research. Subject Editor H. Jiang.

J. B. Azad, I. Rezadad, and R. E. Peale are with the Department of Physics, University of Central Florida, Orlando, FL 32816 USA (e-mail: javaneh@knights.ucf.edu; imen@knights.ucf.edu; robert.peale@ucf.edu).

J. W. Cleary and K. Eyink are with the Air Force Research Laboratory, Wright-Patterson Air Force Base, Dayton, OH 45433 USA (e-mail: justin.cleary.1@us.af.mil; kurt.eyink@us.af.mil).

Color versions of one or more of the figures in this paper are available online at http://ieeexplore.ieee.org.

Digital Object Identifier 10.1109/JMEMS.2015.2463096

II. Experimental Details

Polyimide is usually supplied commercially as polyamic acid precursors dissolved in an N-methyl-2-pyrrolidone (NMP) based solvent suitable for spin coating [23]. The polyimide studied here was ProLift100 (Brewer Science) [27], [28]. This contains 70-90% N-Methyl-2-pyrrolidone (NMP, C5H9NO), which suspends and dilutes the remaining 10-30% polymer solid [29]. NMP has relative molecular mass 99.13, density 1.028 g/cm3, melting point −23 to −24.4 °C, boiling point 202 °C at 101.3 Pa, and vapor pressure 45 Pa at 25 °C [30].

ProLift 100 is advertised as soluble in positive resist developers. We found that it can be co-developed with both positive and negative resists that have Tetra-methyl-ammonium hydroxide (TMAH)-based developer, such as MF319 (MicroChem Corp.), RD6 (Futurrex Inc.), etc. It is resistant to acids and organic solvents. Four-types of ProLift 100 provide different spin-on thickness ranges. Investigated in this work was a ProLift 100-20, which is 80% NMP and 20% solid [28]. This particular spin-on ProLift typically results in thicknesses in the range 1-4 micrometers, according to manufacturer specifications.

ProLift was spun on at 1800 rpm for 90 sec, soft baked at 150 °C for 90 sec, and hard baked at 300 °C for 180 sec, to produce a ∼1.8 μm layer, as determined by profilometry. Similarly a ∼2 μm ProLift layer was produced by 1500 rpm spin and identical baking recipe. However, we obtained better uniformity over 75 mm wafers by spinning at 500 rpm for 5 sec, 1000 rpm for 10 sec, 0 rpm for 10 sec, and 3000 rpm for 90 sec, followed by soft baking at 120 °C for 90 sec and hard baking at 300 °C for 90 sec, which gave a layer thickness of 1.2 μm.

We prepared a MEMS cantilever device, which was designed for IR sensing, using eight mask steps [31]. The main structure of the device was made by sequences of oxide and metal depositions and patterning. Oxide depositions were done by plasma-enhanced chemical vapor deposition (PECVD) and metal depositions by electron-beam evaporation. The cantilever was made on top of 2 μm of spin-coated ProLift sacrificial layer which was paired with a layer of positive photoresist to create patterned anchor vias through the ProLift by photolithography and co-development. Similarly, a divot (partial via) was patterned in the ProLift for depositing a metal tip contact using negative photo resist (NR9-1500)

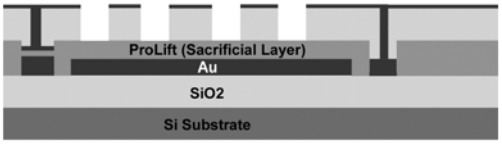

Fig. 1. Schematic of fabricated MEMS cantilever before removal of sacrificial layer. Scales are exaggerated for presentation purposes.

TABLE I
DRY ETCH RECIPES FOR RELEASING CANTILEVER STRUCTURE FROM PROLIFT

Recipe	RF Power (W)	Pressure (mTorr)	O2 flow (sccm)	CF4 flow (sccm)
A	100	900	98	4
B	150	750	98	4
C	150	400	50	4

TABLE II
THERMAL TREATMENTS APPLIED TO PROLIFT

	α	β	γ
Soft bake 110-150 °C, 90 sec	X	X	X
Hard bake 200-300 °C, 90-180 sec	X	X	X
PECVD 300 °C, 30 min		X	X
Soft bake 110-150 °C, 10 min			X

on top of the sacrificial layer. Next a PECVD silicon-oxide layer was grown on top of the ProLift using a Trion Orion II system with Tetraethyl orthosilicate (TEOS) precursor. During growth, the ProLift was heated at 300 °C for 30 minutes. The cantilever pattern was created on top of deposited oxide by another metal deposition and lift off. This metallic pattern served as a mask to transfer the cantilever pattern to the underlying oxide using a Trion Minilock II reactive ion etcher. The resulting structure comprised a 100 μm^2 oxide paddle with metallic top surface. The paddle was supported by $\sim$100 μm long U-shaped oxide arms, whose 8 μm and 10 μm wide sections were joined at their ends opposite the paddle by an elbow. One of the arms was connected to the paddle and the end of the other arm was connected to the substrate via the anchor. A few 10 μm diameter holes were patterned in the paddle to assist the release [5]–[7], [23], [32], [33]. A schematic of the structure is presented in Fig. 1.

Finally, the sacrificial layer was removed. This final release step is the subject of this paper. Dry release was done using the Trion Minilock II RIE according to recipes given in Table 1. Adding CF_4 to an O_2 plasma considerably increased the etch rate of polyimide and helped to eliminate polymer "grass" on the substrate [37]–[40].

The integrated thermal histories for the ProLift investigated here are summarized in Table 2, which defines baking treatments α, β, and γ. Treatment α refers to the regular photolithography baking process in which spun ProLift is soft-baked on a hotplate at 120-150 °C for 90 seconds and hard-baked at 200-300 °C for 90-180 seconds.

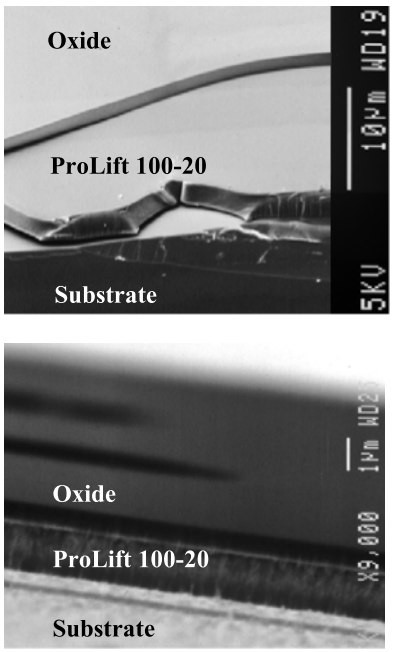

Fig. 2. (Top) SEM image of PECVD oxide on spin-coated ProLift on silicon. (Bottom) Cross-sectional view of oxide cantilever on ProLift sacrificial layer.

Treatment β adds an additional 30 min baking at 300 °C during PECVD. Treatment γ adds a couple of photoresist baking steps, all in the range of 110 - 150 °C, before and after oxide deposition in order to complete the device.

UV exposure was performed using our mask aligner. The HSA350 mercury short-arc lamp provides 10 mW/cm^2 intensity at the sample. Intensity was determined by an OAI MIMIR Hybrid Technology 100 optical power meter.

Reflectivity spectra were measured using a Perkin-Elmer UV-Visible spectrometer on ProLift samples that had been spun onto silver-coated silicon substrates. The optical constants n and κ for ProLift were determined using a J. A. Woollam V-Vase ellipsometer. The WVASE32 modeling software accounts for the bare-silicon substrate of the samples prepared for ellipsometry. The reflectivity spectrum is given in terms of the optical constants by

$$R \cong R_0 + (1 - R_0)^2 \exp[-\frac{8\pi\kappa d}{\lambda}] \quad (1)$$

where

$$R_0 = \left|\frac{1 - n + i\kappa}{1 + n + i\kappa}\right|^2 \quad (2)$$

is the reflectivity at the front surface due to the discontinuity in permittivity. Absorptance A = 1-R gives the fraction of incident UV light that is absorbed by the ProLift, considering two passes through thickness d, neglecting multiple reflections, and assuming perfect reflectance from the substrate at all wavelengths.

III. RESULTS

Fig. 2 (top) presents a scanning electron microscope (SEM) image of a $\sim$1 μm layer of SiO2 supported by $\sim$2 μm of

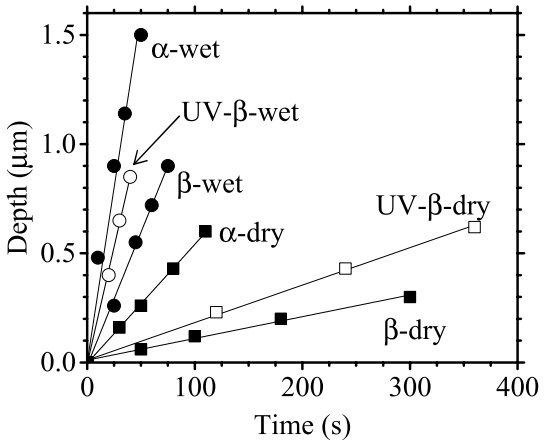

Fig. 3. (Solid symbols) Comparison of wet and dry etch rates for α and β baked ProLift, and (open symbols) for β-ProLift after UV exposure.

ProLift "β" on a silicon substrate. Our MEMS structures are patterned in such oxide and then released from the ProLift.

Fig. 2 (bottom) presents an oblique-angle SEM image of the edge and top of the cantilever paddle after a dry etch has removed the surrounding ProLift "γ". ProLift remains under the paddle. Two release holes are observed on the top of the paddle in the upper left of the image.

Although ProLift 100 is specified to withstand temperatures exceeding 300 °C, we found that removal becomes more and more difficult the longer it is baked, even at temperatures below this limit. Figure 3 (solid symbols) compares wet and dry etch between two different treatments of α and β. Our experiments reveal little difference in the release behavior for β and γ treatments, in agreement with ProLift's rating to withstand such low temperatures as comprise the additional heat treatments in the γ process. In contrast, the solid symbols in Fig. 3 show that β-ProLift wet etches 2.4 times more slowly than α (2% TMAH; 100 μm lateral dimension; 1.5 μm thickness). For dry etch, the difference is a factor of 5.5 (etch recipe B; thickness 1.2 μm). The open symbols in Fig. 3 are described below.

Complete wet release of the paddle requires an hour, which is longer than predicted by Fig. 3 because of the very small gap between cantilever and substrate. Different solvents were tried for wet-release of β-ProLift, including MF319 (containing 2% TMAH), 5% TMAH solvent, and ProLift remover (Brewer Science). In all cases, the ProLift β came off in slabs like "ice-floes". These migrated on the surface, even without intentional agitation, and collided with the cantilevers, shearing them off. An optical microscope image of free floating ProLift slabs and a damaged cantilever is presented in Fig. 4. The cantilever has been sheared from its anchors by a floating ProLift island, which is visible on top of the contact pad.

Dry release of β-ProLift with recipe A takes so long that the oxide becomes damaged by physical bombardment from plasma ions, as shown in Fig. 5 [39], [41]. Here the cantilever arms appear badly eroded while the paddle is still incompletely released.

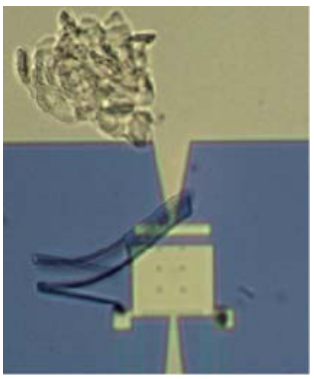

Fig. 4. Optical microscope image of cantilever during wet release. The cantilever has been sheared off by a floating ProLift sheet.

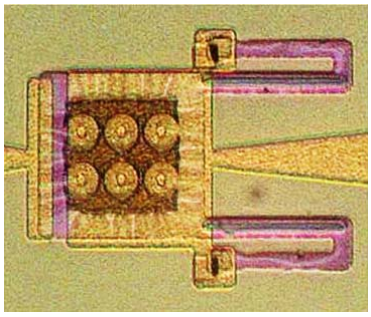

Fig. 5. A cantilever partially released from ProLift β sacrificial layer by 55 minutes of oxygen plasma etch. The cantilever arms have been eroded by ion bombardment.

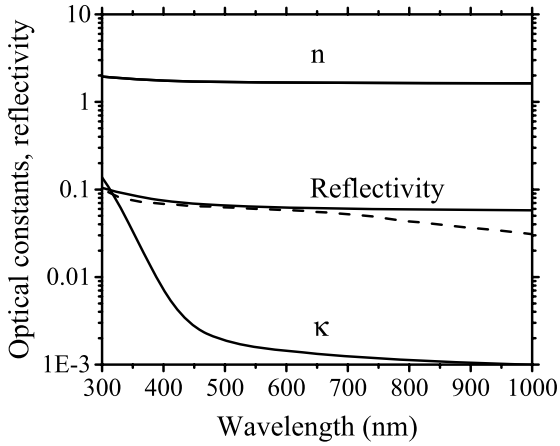

Fig. 6. Refractive index n and extinction coefficient κ for ProLift and the theoretical (solid line) and measured (dash line) R spectrum.

UV exposure speeds both wet and dry etch of ProLift and solves the release problem [31]. To estimate the useful UV dose and spectrum, we determined the ProLift optical properties in the 300-1000 nm range. Fig. 6 presents the measured optical constants. The real part n of the refractive index has the value of ~1.8 throughout the near-UV to near-IR spectral range, and the uncertainty determined from multiple measurements on multiple samples is ~1%. The imaginary part κ rises by 2 orders of magnitude from 600 to 300 nm wavelength, with the uncertainty at long wavelengths

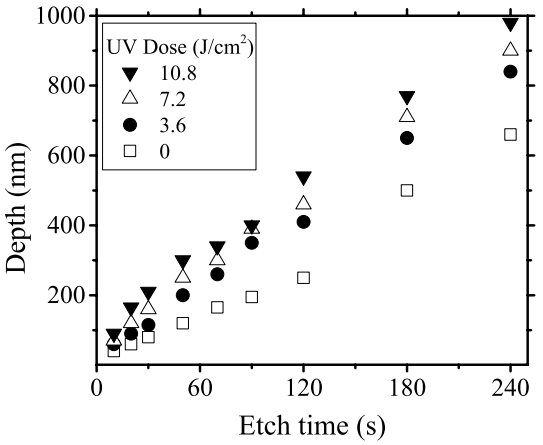

Fig. 7. Dry plasma etch depth vs. time for 1.5 μm thick, 5 mm pattern size hard-baked (β-treatment) ProLift with different UV doses.

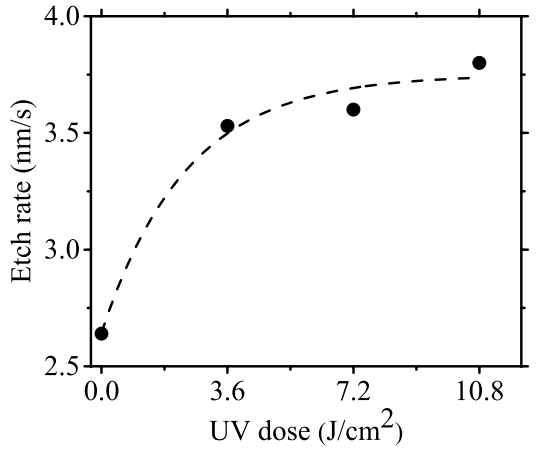

Fig. 8. Dry etch rate (symbols) vs. UV dose and fit to exponential function (dashed line).

where κ is only ~10-3 being ~30%. The measured reflectivity spectrum is also plotted. It confirms the theoretical spectrum calculated from Eq. (1) in the short-wave part of the spectrum, which is the range of most importance to this work. The factor-of-2 disagreement at the longest wavelengths may be due to the neglect of multiple reflections in the calculated spectrum, which become more important where the absorption is small, or large percentage uncertainty for very low values of κ. According to these spectra the characteristic absorption length at the 365 nm emission wavelength of our mask aligner is 1.45 μm, which confirms that ProLift sufficiently absorbs our available UV and to sufficient depths.

Fig. 7 presents a plot of the dry etch depth as a function of UV dose for β-ProLift, which was prepared on a wafer that was cleaved into four smaller pieces for the different UV exposures. These four pieces were subsequently subdivided in to nine small pieces for different etch durations. For these experiments only, we used the Samco RIE with 50 W power, 53 mTorr pressure, and 5 sccm O2 flow rate, which is not included as one of the recipes in Table I. The highest UV dose gives the highest initial etch rate.

Fig. 8 presents a plot of dry-etch rate r as a function of UV dose D for β-ProLift. The etch rate is determined from

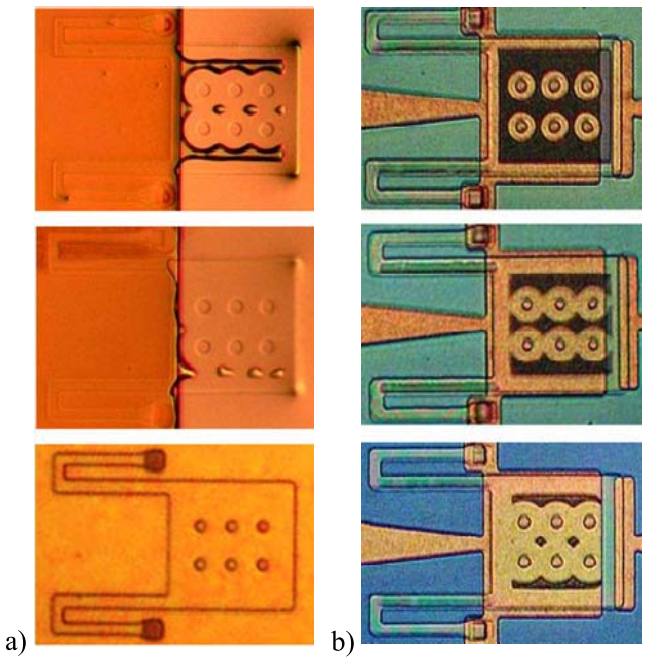

Fig. 9. (a) (Top) partially released paddle after 12 minutes in MF319 developer, while arms and anchors are covered by PR. (Middle) Paddle is almost released after 22 minutes in MF319 with PR still present. (Bottom) PR is stripped and the whole cantilever is soaked in fresh MF319 developer, fully releasing the cantilever after 13 minutes. (b) (Top to bottom) Optical microscope images of the stages of cantilever release after 60, 90, and 120 minutes O_2 plasma etch.

the Fig. 7 data by the depth after 240 seconds, assuming linear behavior. The etch rate saturates above 3600 mJ/cm2. The line is a fit of the function $r = r_0 + (r_s - r_0)(1\text{-}\exp[-D/D_0])$ to the data. The parameters obtained from the fit are $r_0 = 2.64$ nm/s for the unexposed etch rate, $r_s = 3.75$ nm/s for the saturated rate, and $D_0 = 4.05$ J/cm^2 for the characteristic dose. The saturated rate is 1.42 times faster than the unexposed rate. This proved to be enough of an improvement to overcome the release problems revealed in Figs. 4 and 5.

The open symbols in Fig. 3 represent wet and dry etch depths vs. time for β-ProLift after a UV exposure of 3600 mJ/cm2. This dose is close to the characteristic saturation dose determined from Fig. 8 for a different set of dry etch data using etch recipe C, Table 1. UV exposed β-ProLift wet-etches 1.76 times faster than unexposed β-ProLift. Similarly, the dry etch rate for the exposed β-ProLift is 1.34 faster, which is the about the same factor as for the data in Fig. 8. However, UV fails to fully recover the etch rate of β-ProLift to the rate of unexposed α-ProLift, which was not hard-baked.

In fabricating our cantilever devices, we exposed ProLift γ to 3600 mJ/cm^2 UV after etching the oxide. Then the sample was dry etched until the ProLift surrounding the cantilevers was gone. This allowed subsequent wet release by eliminating the possibility for large slabs to break free and bulldoze the cantilevers. A layer of photoresist was deposited and patterned to cover the delicate arms and anchors during the wet release of the paddles in MF319 developer. Then we stripped the PR and placed our sample into a dish of fresh MF319 to release

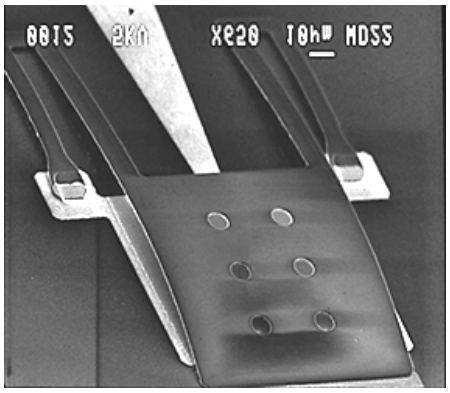

Fig. 10. SEM image of released downward-curling structure. Magnification is 650X.

the arms. Optical microscope images of the intermediate steps in this sequential wet release approach are presented in Fig. 9 (column a). Wet etch gave low yield due to stiction [9], [25], [26], [32], [42], [43].

We achieved 90% fabrication yield without bombardment damage using dry oxygen plasma etch after UV exposure which is 200 % improvement compared to 30% fabrication yield for devices released without UV exposure. Moreover, the substrate surrounding the cantilevers was cleaner and had much less residue compared to its condition after wet release. Fig. 9 (column b) presents optical microscope images of the intermediate steps in the dry release. Etching was done using the Trion Minilock II RIE using recipe A (Table I).

Fig. 10 presents an SEM image of a fully released device. The downward curvature with touching tip is as desired for intended function [34], [44], [45].

IV. Conclusion

Removal of polyimides that are used as sacrificial layer in fabricating MEMS devices can be challenging after hard-baking, which may easily result by the end of multiple-step processing. UV exposure allowed rapid dry etch of the ProLift surrounding the oxide cantilevers, which eliminated the risk of large floating sheets sheering the cantilevers from their anchors. Then the remaining ProLift under the cantilevers could be easily removed by either wet developer or by additional oxygen plasma etch without risk of damaging the cantilevers. This method provided significant increase of 200% in fabrication yield for our devices.

References

[1] H. U. Rahman, "Plasma based dry release of MEMS devices," in *Microelectromechanical Systems and Devices*. Rijeka, Croatia: InTech, 2012, ch. 11, pp. 269–290.

[2] A. Kshirsagar, S. P. Duttagupta, and S. A. Gangal, "Optimisation and fabrication of low-stress, low-temperature silicon oxide cantilevers," *IET Micro Nano Lett.*, vol. 6, no. 7, pp. 476–481, Jul. 2011. [Online]. Available: http://digital-library.theiet.org/content/journals/10.1049/mnl.2011.0076;jsessionid=1g277cr4rtibd.x-iet-live-01

[3] A. B. Graham *et al.*, "A method for wafer-scale encapsulation of large lateral deflection MEMS devices," *J. Microelectromech. Syst.*, vol. 19, no. 1, pp. 28–37, Feb. 2010. [Online]. Available: http://ieeexplore.ieee.org/xpl/articleDetails.jsp?arnumber=5340675

[4] N. Behnel, T. Fuchs, and H. Seidel, "A new highly selective sacrificial layer technology for SiC MEMS," in *Proc. 15th Int. Conf. Solid-State Sens., Actuators, Microsyst.*, Denver, CO, USA, Jun. 2009, pp. 740–742.

[5] S. Mouaziz, G. Boero, R. S. Popovic, and J. Brugger, "Polymer-based cantilevers with integrated electrodes," *J. Microelectromech. Syst.*, vol. 15, no. 4, pp. 890–895, Aug. 2006. [Online]. Available: http://ieeexplore.ieee.org/xpl/articleDetails.jsp?arnumber=1668185

[6] D. Grbovic *et al.*, "Uncooled infrared imaging using bimaterial microcantilever arrays," *Appl. Phys. Lett.*, vol. 89, no. 7, p. 073118, Aug. 2006. [Online]. Available: http://scitation.aip.org/content/aip/journal/apl/89/7/10.1063/1.2337083

[7] S. R. Hunter, G. Maurer, L. Jiang, and G. Simelgor, "High-sensitivity uncooled microcantilever infrared imaging arrays," *Proc. SPIE*, vol. 6206, p. 62061J, May 2006.

[8] M. Almasri, Z. Celik-Butler, D. P. Butler, A. Yaradanakul, and A. Yildiz, "Uncooled multimirror broad-band infrared microbolometers," *J. Microelectromech. Syst.*, vol. 11, no. 5, pp. 528–535, Oct. 2002. [Online]. Available: http://ieeexplore.ieee.org/xpl/articleDetails.jsp?arnumber=1038848

[9] S. Frederico, C. Hibert, R. Fritschi, P. Fluckiger, P. Renaud, and A. M. Ionescu, "Silicon sacrificial layer dry etching (SSLDE) for free-standing RF MEMS architectures," in *Proc. IEEE 16th Annu. Int. Conf. Micro Electro Mech. Syst.*, Kyoto, Japan, Jan. 2003, pp. 570–573.

[10] C. L. Roozeboom *et al.*, "Integrated multifunctional environmental sensors," *J. Microelectromech. Syst.*, vol. 22, no. 3, pp. 779–793, Jun. 2013. [Online]. Available: http://ieeexplore.ieee.org/xpl/articleDetails.jsp?arnumber=6484867

[11] F. Jiang, A. Keating, M. Martyniuk, R. Pratap, L. Faraone, and J. M. Dell, "Process control of cantilever deflection for sensor application based on optical waveguides," *J. Microelectromech. Syst.*, vol. 22, no. 3, pp. 569–579, Jun. 2013. [Online]. Available: http://ieeexplore.ieee.org/xpl/articleDetails.jsp?arnumber=6399504

[12] S. Sha-Li, C. Da-Peng, J. Yu-Peng, O. Yi, Y. Tian-Chun, and X. Qiu-Xia, "A novel method for sacrificial layer release in MEMS devices fabrication," *Chin. Phys. B*, vol. 19, no. 7, p. 076802, Jul. 2010. [Online]. Available: http://iopscience.iop.org/1674-1056/19/7/076802/

[13] C. Li *et al.*, "A novel uncooled substrate-free optical-readable infrared detector: Design, fabrication and performance," *Meas. Sci. Technol.*, vol. 17, no. 7, p. 1981, Jul. 2006. [Online]. Available: http://iopscience.iop.org/0957-0233/17/7/042/

[14] G. K. Fedder *et al.*, "Laminated high-aspect-ratio microstructures in a conventional CMOS process," in *Proc. 9th IEEE Annu. Int. Conf. Micro Electro Mech. Syst.*, San Diego, CA, USA, Feb. 1996, pp. 13–18.

[15] A. Bagolini, L. Pakula, T. L. M. Scholtes, H. T. M. Pham, P. J. French, and P. M. Sarro, "Polyimide sacrificial layer and novel materials for post-processing surface micromachining," *J. Microelectromech. Syst.*, vol. 12, no. 4, p. 385. Jul. 2002. [Online]. Available: http://iopscience.iop.org/0960-1317/12/4/306/

[16] A. Bogozi *et al.*, "Elastic modulus study of gold thin film for use as an actuated membrane in a superconducting RF MEM switch," *IEEE Trans. Appl. Supercond.*, vol. 15, no. 2, pp. 980–983, Jun. 2005. [Online]. Available: http://ieeexplore.ieee.org/xpl/articleDetails.jsp?arnumber=1439804

[17] M. G. Allen, "A fully integrated micromachined toroidal inductor with a nickel-iron magnetic core (the switched dc/dc converter application)," in *Proc. 7th Int. Conf. Solid-State Sens. Actuators*, Yokohama, Japan, 1993, pp. 70–73.

[18] W. Wang, V. Upadhyay, J. Bumgarner, and O. Edwards, "Simulation and experimental studies of an uncooled MEMS capacitive infrared detector for thermal imaging," *J. Phys., Conf. Ser.*, vol. 34, no. 34, p. 350, 2006. [Online]. Available: http://iopscience.iop.org/1742-6596/34/1/057

[19] H. U. Rahman and R. Ramer, "Dry release of MEMS structures using reactive ion etching technique," in *Proc. 3rd IEEE Int. Symp. Microw., Antenna, Propag. EMC Technol. Wireless Commun.*, Beijing, China, Oct. 2009, pp. 517–520.

[20] R. Amantea, C. M. Knoedler, F. P. Pantuso, V. K. Patel, D. J. Sauer, and J. R. Tower, "Uncooled IR imager with 5-mK NEDT," *Proc. SPIE*, vol. 3061, p. 210, Aug. 1997.

[21] R. Amantea *et al.*, "Progress toward an uncooled IR imager with 5-mK NETD," *Proc. SPIE*, vol. 3436, p. 647, Oct. 1998.

[22] C.-W. Baek, Y.-K. Kim, Y. Ahn, and Y.-H. Kim, "Measurement of the mechanical properties of electroplated gold thin films using micromachined beam structures," *Sens. Actuators A, Phys.*, vol. 117, no. 1, pp. 17–27, Jan. 2005. [Online]. Available: http://www.sciencedirect.com/science/article/pii/S0924424704001177

[23] S. Ma, Y. Li, X. Sun, X. Yu, and Y. Jin, "Study of polyimide as sacrificial layer with O_2 plasma releasing for its application in MEMS capacitive FPA fabrication," in *Proc. Int. Conf. Electron. Packag. Technol. High Density Packag.*, Beijing, China, Aug. 2009, pp. 526–529.

[24] M. Hu, J. Chen, Z. Lai, H. Mao, and D. Sheng, "Research for polyimide as a sacrificial layer in MEMS device," *Proc. SPIE*, vol. 5774, p. 642, Dec. 2004.

[25] X. Guo, M. Cai, L. Liu, Z. Lai, and S. Zhu, "A novel method of removing polyimide sacrificial layer," in *Proc. 1st IEEE Int. Conf. Nano/Micro Eng. Molecular Syst.*, Zhuhai, China, Jan. 2006, pp. 209–212.

[26] H.-S. Hwang and J.-T. Song, "An effective method to prevent stiction problems using a photoresist sacrificial layer," *J. Micromech. Microeng.*, vol. 17, no. 2, p. 245, Feb. 2007. [Online]. Available: http://iopscience.iop.org/0960-1317/17/2/009/

[27] M. Lai, G. Parish, Y. Liu, J. M. Dell, and A. J. Keating, "Development of an alkaline-compatible porous-silicon photolithographic process," *J. Microelectromech. Syst.*, vol. 20, no. 2, pp. 418–423, Apr. 2011. [Online]. Available: http://ieeexplore.ieee.org/xpl/articleDetails.jsp?arnumber=5719146

[28] M. Lai, G. M. Sridharan, G. Parish, S. Bhattacharya, and A. Keating, "Multilayer porous silicon diffraction gratings operating in the infrared," *Nanosc. Res. Lett.*, vol. 7, no. 1, p. 645, Nov. 2012. [Online]. Available: http://www.nanoscalereslett.com/content/7/1/645

[29] *Prolift 100 Series. Manufacturer*, Brewer Science, Inc., Vichy, MO, USA, 2005.

[30] B. Akesson, *N-Methyl-2-Pyrrolidone*, World Health Organization, Geneva, Switzerland, document 35, 2001.

[31] J. B. Azad, I. Rezadad, J. Nath, E. Smith, and R. E. Peale, "Release of MEMS devices with hard-baked polyimide sacrificial layer," *Proc. SPIE*, vol. 8682, p. 868226, Mar. 2013.

[32] S. Huang and X. Zhang, "Application of polyimide sacrificial layers for the manufacturing of uncooled double-cantilever microbolometers," in *Proc. MRS*, vol. 890. Boston, MA, USA, 2005, p. 125.

[33] M. Shahriar Rahman, M. M. Chitteboyina, D. P. Butler, Z. Celik-Butler, S. P. Pacheco, and R. V. McBean, "Device-level vacuum packaging for RF MEMS," *J. Microelectromech. Syst.*, vol. 19, no. 4, pp. 911–918, Jul. 2010. [Online]. Available: http://ieeexplore.ieee.org/xpl/articleDetails.jsp?arnumber=5508328

[34] I. Rezadad, J. Boroumand, E. M. Smith, and R. E. Peale, "Micro electro mechanical cantilever with electrostatically controlled tip contact," *Appl. Phys. Lett.*, vol. 105, no. 3, p. 033514, Jul. 2014. [Online]. Available: http://scitation.aip.org/content/aip/journal/apl/105/3/10.1063/1.4891496

[35] I. Rezadad, J. Boroumand, E. M. Smith, A. Alhasan, and R. E. Peale, "Vertical electrostatic force in MEMS cantilever IR sensor," *Proc. SPIE*, vol. 9070, p. 90701U, Jun. 2014.

[36] J. Boroumand, I. Rezadad, A. Alhasan, E. M. Smith, and R. E. Peale, "Thermomechancial characterization in a radiant energy imager using null switching," *Proc. SPIE*, vol. 9070, p. 907020, Jun. 2014.

[37] W. E. Vanderlinde, C. J. Von Benken, and A. R. Crockett, "Rapid integrated circuit delayering without grass," *Proc. SPIE*, vol. 2874, p. 260, Sep. 1996.

[38] F. D. Egitto, F. Emmi, R. S. Horwath, and V. Vukanovic, "Plasma etching of organic materials. I. Polyimide in O_2–CF_4," *J. Vac. Sci. Technol. B*, vol. 3, no. 3, p. 893, Jan. 1985. [Online]. Available: http://scitation.aip.org/content/avs/journal/jvstb/3/3/10.1116/1.583078

[39] U. Buder, J.-P. von Klitzing, and E. Obermeier, "Reactive ion etching for bulk structuring of polyimide," *Sens. Actuators A, Phys.*, vol. 132, no. 1, pp. 393–399, Nov. 2006. [Online]. Available: http://www.sciencedirect.com/science/article/pii/S0924424706002962

[40] D. L. Flamm and V. M. Donnelly, "The design of plasma etchants," *Plasma Chem. Plasma Process.*, vol. 1, no. 4, pp. 317–363, Dec. 2006. [Online]. Available: http://link.springer.com/article/10.1007/BF00565992

[41] A. Yildiz, Z. Celik-Butler, and D. P. Butler, "Microbolometers on a flexible substrate for infrared detection," *IEEE Sensors J.*, vol. 4, no. 1, pp. 112–117, Feb. 2004. [Online]. Available: http://ieeexplore.ieee.org/xpl/articleDetails.jsp?arnumber=1261870

[42] H. T. M. Pham *et al.*, "Polyimide sacrificial layer for an all-dry post-process surface micromachining module," in *Proc. 12th Int. Conf. Solid-State Sens., Actuators, Microsyst.*, Boston, MA, USA, Jun. 2003, pp. 813–816.

[43] C. H. Mastrangelo, "Suppression of stiction in MEMS," in *Proc. MRS*, vol. 605. Boston, MA, USA, 1999, p. 105.

[44] O. Edwards, "Radiant energy imager using null switching," U.S. Patent 7 977 635, Jul. 12, 2011. [Online]. Available: http://www.google.com/patents/US7977635

[45] E. Smith *et al.*, "MEMS clocking-cantilever thermal detector," *Proc. SPIE*, vol. 8704, p. 87043B, Jun. 2013.

Authors' photographs and biographies not available at the time of publication.